
**ELECTRONIC PROPERTIES
OF SEMICONDUCTORS**

Anticorrelation between the Intensity of Stimulated Picosecond Emission in GaAs and the Characteristic Time of Charge-Carrier Cooling

N. N. Ageeva^a, I. L. Bronevoi^{a,*}, D. N. Zabegaev^a, and A. N. Krivonosov^a

^a Kotel'nikov Institute of Radio Engineering and Electronics, Russian Academy of Sciences, Moscow, 125009 Russia

*e-mail: bil@cplire.ru

Received July 10, 2019; revised August 5, 2019; accepted August 20, 2019

Abstract—During the powerful picosecond optical pumping, intense stimulated picosecond emission arises in a thin GaAs layer. It is found that, first, the maximum emission intensity decreases as the diameter of the pump beam increases (while the pump energy density is fixed). Second, this dependence anticorrelates with the dependence of the characteristic relaxation time of the emission on the beam diameter. This time is related to the characteristic cooling time of charge carriers, which is slowed due to carrier heating by emission. This leads to the anticorrelation given in the title.

Keywords: stimulated picosecond emission, charge-carrier cooling, gain saturation, Beer–Lambert–Bouguer law

DOI: 10.1134/S1063782620010029

1. INTRODUCTION

Intrinsic stimulated (amplified spontaneous) picosecond emission arises in a thin layer of GaAs when it is subjected to picosecond optical pumping. For brevity, below we refer to simply “emission”. Pumping the charge carriers leads at the same time to bleaching of the layer, i.e., to an increase in its transparency. The relaxation of emission and bleaching at the trailing edge of the pump pulse and after the end of the pulse was considered in [1]. The relaxation of bleaching reflects predominantly the relaxation of the charge-carrier density. It was established that the characteristic relaxation time of bleaching and emission is related to the characteristic time τ_T of carrier temperature relaxation. This observation became the starting point for studying the relation between the emission intensity and the time τ_T described in this paper. Here, we investigate the variation in the emission intensity and time τ_T with an increase in the diameter D of the pump beam. We find that the observed variation in the emission intensity is opposite to that expected from the Bouguer law for the active region, valid in linear optics. We note that the variation in the emission intensity with an increase in the length of the active region under so-called gain saturation, i.e., in the case where the emitted radiation affects the process of its own amplification, was analyzed earlier, e.g., in [2, 3]. However, this was done for the steady-state situation and for other conditions that are different from the case under study, and that work was largely mathemat-

ical. Therefore, the effect described in this paper went unnoticed.

2. EXPERIMENTAL

The experiments were carried out at room temperature T_R using a picosecond laser spectrophotometric complex with an automated measurement system (Fig. 1). The complex consists of a PL PDP1-300 diode-pumped YAG master laser oscillator; a system of laser-pulse amplifiers pumped by 700TC series power supplies; light-pulse frequency doublers (KDP crystals); two LiNbO₃-based optical parametric oscillators with temperature wavelength tuning, one of them used to produce pump pulses and the other to produce probe or other pulses with a duration of about 10 ps FWHM and linear polarization; and a spectrophotometric system. The most important components of the latter are a SpectraPro-2500i double spectrograph used for both spectral measurements and (in the dispersion subtraction mode) as a bandpass wavelength filter that leaves the emission pulse duration undistorted; a PS-1/S1 picosecond streak camera; and PIXIS and CoolSNAP:HQ2 CCD cameras that record, respectively, the emission spectrum and the temporal behavior of the intensity of the emission spectral component passed by the spectrograph.

The sample under study is an Al_{0.32}Ga_{0.68}As/GaAs/Al_{0.32}Ga_{0.68}As heterostructure

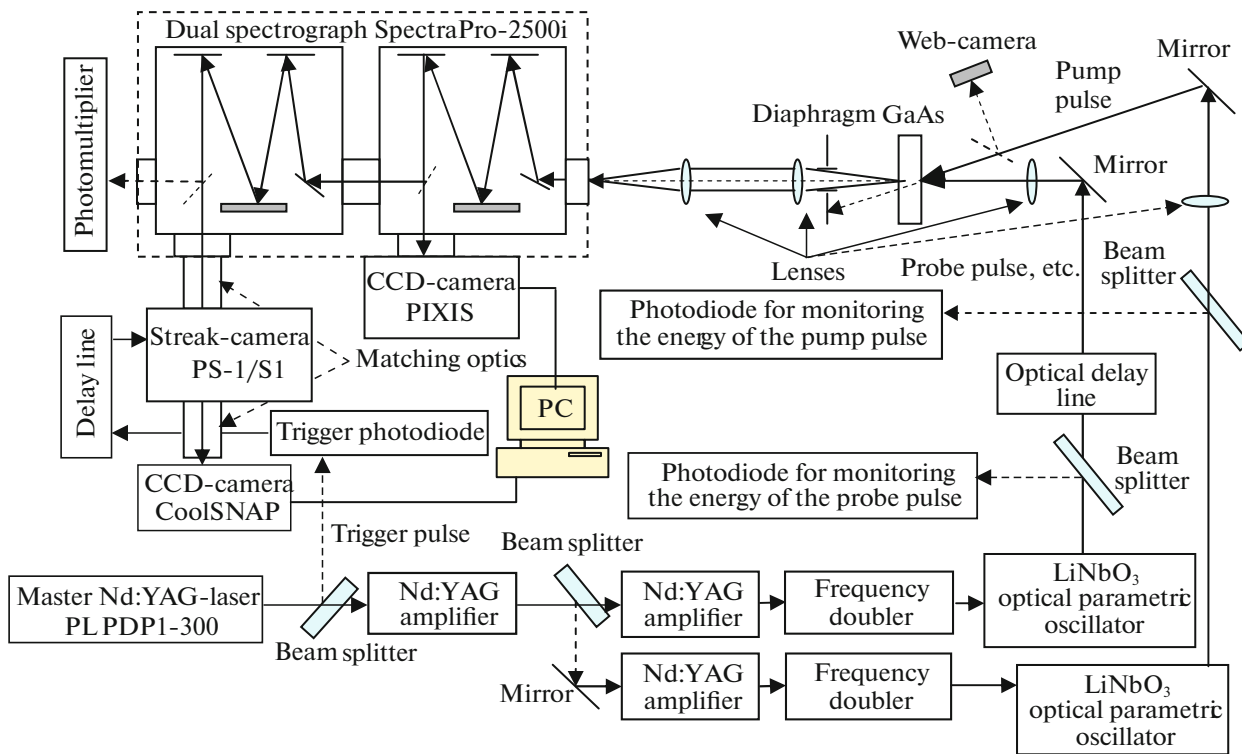


Fig. 1. Layout of the laser picosecond spectrophotochronometric complex.

with layer thicknesses of 1.2, 1.6, and 1.3 μm , respectively. The $\text{Al}_x\text{Ga}_{1-x}\text{As}$ layers are transparent for the light used in the experiments. The sample surfaces (apart from the edge ones) had an antireflection coating.

Radiation emitted in the optically pumped region of the GaAs layer is amplified there in the direction along the layer. The diameter of the pump beam D at the sample location was successively changed from 0.2 to 1.1 mm FWHM. The cross-sectional distribution of the light intensity in the pump beam was approximately Gaussian. For all values of D , the pump energy density W_{ex}/V was kept constant (here, W_{ex} is the pump pulse energy, $V = \pi D^2 l / 4$ is the volume of the pumped region, and l is the thickness of the GaAs layer). Due to the antireflective coating, the reflection of pump light from the sample surface did not exceed 2%. The diameter D was measured by diverting the beam to a web camera by means of a movable mirror and analyzing the recorded image (Fig. 1). The web camera was located at the same distance from the mirror as the sample under study.

Measurements of the sample transparency for pump pulses with diameters of $D = 0.2$ and 1.1 mm indicated that the density of the pump-pulse energy absorbed in the sample varies by a mere 2%; i.e., it is almost independent of D . According to our estimates, the rate of stimulated recombination is much higher than the rate of other recombination processes [1].

Taking this into account, the total energy density W_s of emitted radiation should be the same for all values of D and equal to the density of the absorbed pump energy minus the threshold pump energy density. Hereafter, the energy density refers to the energy averaged over the volume V .

Similarly to [1], we carried out measurements of the time-integrated emission spectrum $W(\hbar\omega)$, the envelope shapes of spectrally integrated pump and emission pulses (labeled below by subscripts ex and s, respectively), etc. The plots of the envelopes of the pump and emission pulses measured in real time will be called chronograms and denoted $H_{\text{ex}}(t)$ and $H_s(t)$, respectively.

The part of the emission leaving the pumped region of the layer within a solid angle of 1.2×10^{-2} sr along the axis orthogonal to the heterostructure surface was analyzed. This part of emission was selected for the following reasons. The propagation of light through a material medium should be accompanied by the scattering of this light [4]. Scattering occurs whenever electrons capable of oscillating under the action of an alternating field of the light wave are present in the medium. In our case, these are nonequilibrium electrons produced by the pump. If the medium is optically homogeneous, then, in the first approximation, secondary waves emitted due to electron oscillations will exactly cancel each other for any direction of propagation outside the plane of the GaAs layer.

Because of the presence of optical inhomogeneities (defects) in real media, the mutual cancellation of secondary waves becomes partial rather than complete, so that light becomes scattered in different directions. Let $k < 1$ be the fraction of emission that is scattered (i.e., comes out of the pumped region of the GaAs layer) orthogonally to the layer plane and is measured in the experiment. Radiation emitted in this direction is most suitable for measurements because it exits immediately from the active region and remains unmodified by absorption in the passive region and by reflection from the sample edges. The fact that emission propagating along the epitaxial layer and emission exiting through the heterostructure surface due to its imperfection is the same emission generated due to stimulated emission in the sample was proved in our previous studies, and evidence for this is summarized in [1]. We add that the emission pattern measured in [5] is quite similar to a typical scattering indicatrix, graphically representing the distribution of the scattered light intensity in different directions.

The value of the coefficient k depends, in particular, on the density of defects. The areas under the curves of the emission spectrum $S_{\text{spec}}^V = \frac{1}{V} \int W d(\hbar\omega)$ (a) and the emission chronogram $S_{\text{chr}}^V = \frac{1}{V} \int H_s dt$ (b) normalized to the volume V should be proportional to kW_s . As far as $W_s \approx \text{const}$ in our experiments, the deviation of the functions $S_{\text{spec}}^V = f(D)$ and $S_{\text{chr}}^V = f(D)$ from constant values offers a measure of the spatial inhomogeneity of the defect density and the coefficient k (Fig. 2). The areas of S_{spec}^V and S_{chr}^V remain nearly independent of D for $D > 0.2$ and > 0.36 mm, respectively. Consequently, in this range of D , the defect density averaged over the pumped area of the layer is nearly constant. Some variation in the values of S_{spec}^V and S_{chr}^V , caused by the shift of the pumped spot at the sample, appears for $D \leq 0.2$ and ≤ 0.36 mm, respectively (Fig. 2). Therefore, for such small values of D , the average density of defects varies somewhat in space.

Let us compare the emission intensity for different values of D that would be measured if k were independent of D . The value of this intensity, which we denote by I_s , is related to the actually measured chronograms as $I_s = aH_s/kS$, where $S = \pi D^2/4$ (and a is a coefficient independent of D). Let us take advantage of the fact that the area under the curve of an emission chronogram $S_{\text{chr}} = \int H_s dt$ can be represented as $S_{\text{chr}} = bklSW_s$, where the coefficient b , as well as l and W_s , are constants under the conditions of our experiment. Then, for a comparison independent of k , the emission intensity can be represented in relative units as $I_s = H_s/S_{\text{chr}}$. As an example, Fig. 3 shows the plots of $I_s = f(t)$ for $D = 0.21$

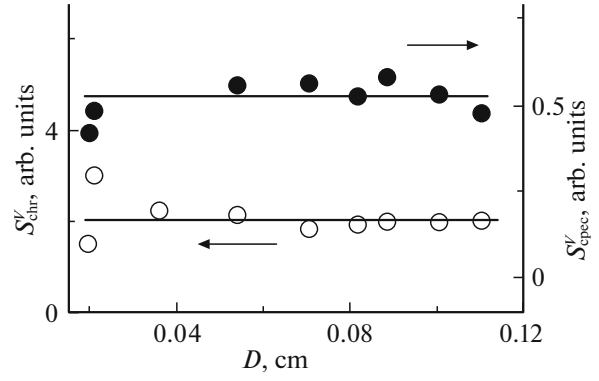


Fig. 2. Areas under curves normalized to the volume V for the emission spectrum and the emission chronogram (S_{spec}^V and S_{chr}^V , respectively) versus the pump-beam diameter D .

and 1.1 mm along with the similarly normalized chronogram of the pump $I_{\text{ex}} = H_{\text{ex}}/S_{\text{ex}} = f(t)$, where $S_{\text{ex}} = \int H_{\text{ex}} dt$ is the area under the curve of the pump chronogram. One can see that the amplitude of $I_s(t)$ (which we denote as $I_{s-\text{max}}$) is higher and emission relaxation is faster for $D = 0.21$ mm in comparison to $D = 1.1$ mm. The observed decrease in the peak emission intensity with an increase in the diameter of the pumped region is illustrated in more detail by the plot of $I_{s-\text{max}}$ as a function of D (see Fig. 4). Only those experimental points for which S_{chr}^V deviate from the mean value (shown by solid line in Fig. 2) by at most 50% were taken into account in Fig. 4. On the trailing edge, emission relaxes with a characteristic time τ_r . The dependence of this relaxation time on D was revealed in [1] and is shown in Fig. 4 by filled circles. Anticorrelation between the dependences of $I_{s-\text{max}}(D)$ and $\tau_r(D)$ can be seen.

3. DISCUSSION OF THE RESULTS

Anticorrelation between the dependences of $I_{s-\text{max}}(D)$ and $\tau_r(D)$ (Fig. 4) means that the maximum emission intensity and the characteristic emission relaxation time are related as

$$I_{s-\text{max}} = \beta/\tau_r, \quad (1)$$

where β is the proportionality coefficient (see Fig. 5, the lower abscissa axis). Supposedly, this anticorrelation can be explained in the following terms.

Because the density and temperature of charge carriers under the conditions of intense emission are related to each other, the time τ_r can be expressed via the characteristic time τ_T of carrier temperature relaxation (i.e., carrier cooling) [1]:

$$\tau_r \approx (2/3)\tau_T. \quad (2)$$

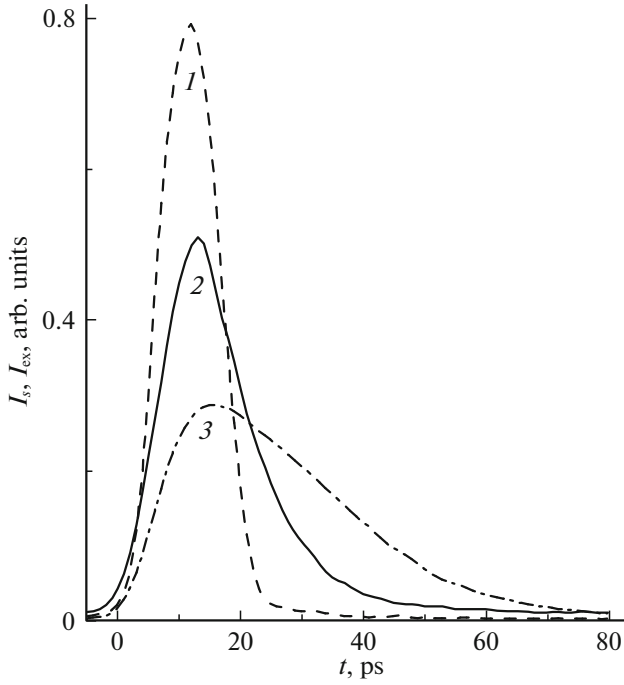


Fig. 3. Normalized chronograms (see text) for (1) the pump pulse $I_{\text{ex}}(t)$ and (2), (3) emission pulse $I_s(t)$ for beam diameters of 0.21 and 1.1 mm, respectively.

When determining τ_T , based on the measured τ_r and Eq. (2), an inversely proportional relationship arises

$$I_{s-\text{max}} = 3\beta/2\tau_T, \quad (3)$$

represented by the same plot in Fig. 5, but with the upper abscissa axis.

It was found in [1] that the measured values of τ_r agree satisfactorily with those estimated by substituting the analytical expression for τ_T obtained in [6] into Eq. (2); this is illustrated in Fig. 4. This expression took into account the slowing down of carrier temperature relaxation due to the heating of carriers by radiation:

$$\tau_T = (A + B\tau_p T_c^{1/2} E_g)\tau_h. \quad (4)$$

Here, $A = 6.3$, $B = 0.4$, and $\tau_h \approx 0.8$ ps is the energy relaxation time of electron–hole plasma via optical-phonon emission taking into account the heating of phonons [7]. The times τ_T , τ_p , and τ_h are expressed in picoseconds; the average carrier temperature T_c is in kelvins; and the band gap E_g is in electronvolts. To obtain better agreement between the calculated and experimental dependences of $\tau_r(D)$ (Fig. 4), the values of A and B are changed slightly with respect to those derived in [6]; we take $A = 6.2$ and $B = 0.34$. The time τ_p is the characteristic time spent by a photon in

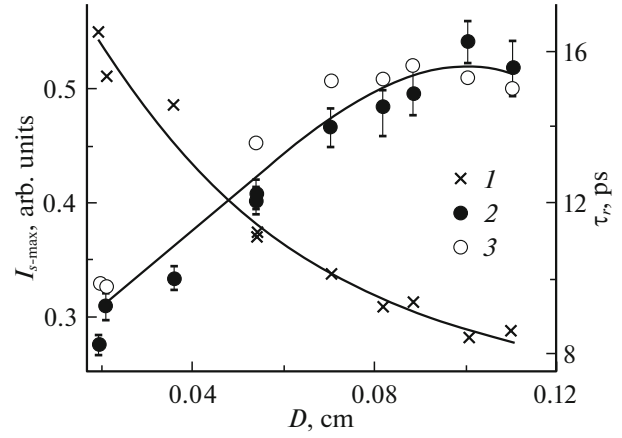


Fig. 4. (1) Maximum emission intensity $I_{s-\text{max}}$ and (2), (3) characteristic emission relaxation time τ_r versus the beam diameter D . Plots (2) and (3) represent the experimental points [1] and calculation results, respectively. Solid lines are drawn as guides to the eye.

the active medium until it leaves this medium or gets absorbed:

$$\tau_p^{-1} \approx c\chi^{-1}(\gamma + D^{-1}). \quad (5)$$

Here, $\chi = 3.6$ is the refractive index of GaAs, $\gamma = \sigma n$ is the coefficient of the intraband absorption of light, and $\sigma = 1.5 \times 10^{-17}$ cm² [8]. Carrying out the estimate, which is described in more detail in [1], in expressions (4) and (5) we used the values of the above parameters corresponding to the average electron den-

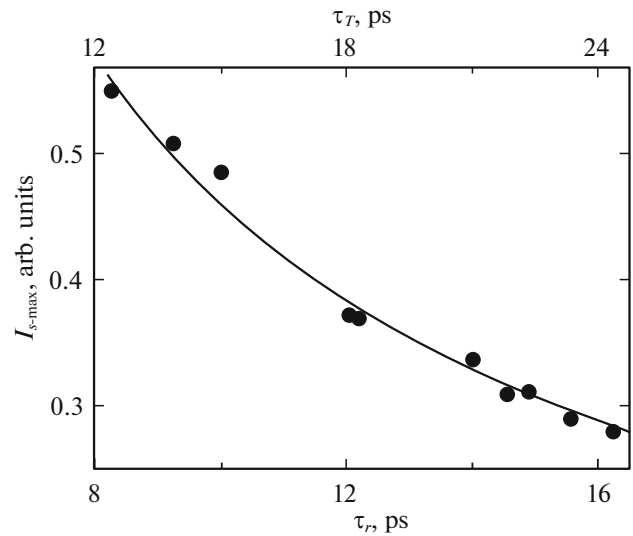


Fig. 5. Maximum emission intensity $I_{s-\text{max}}$ versus the characteristic relaxation times τ_r and τ_T of the emission intensity and the carrier temperature, respectively. The solid line shows the dependence $I_{s-\text{max}} = \beta/\tau_r$ (where β is a constant).

sity $n_{av} = (n_m + n_{th})/2$ during the emission process, where n_{max} and n_{th} are the maximum and the threshold charge-carrier densities, respectively (the threshold is determined by the onset of emission). It should be noted that the density n_{max} was determined for each D from the density-dependent value of the band gap E_g renormalized by Coulomb interaction between the carriers. The value of E_g was determined by the position of the long-wavelength edge of the normalized spectrum $W_n(\hbar\omega) = W(\hbar\omega)/S_{spec}$, where $S_{spec} = \int W d(\hbar\omega)$. Normalizing by S_{spec} (in the same way as we did for chronograms), we bring all spectra to the same values of k and the “emission energy”. Only those experimental points for which S_{spec}^V deviate from the mean value by at most 28% were taken into account.

With increasing D , the carrier density n_{max} decreases, attains a minimum for $D_b \approx 0.7$ mm, and then increases again (Fig. 6). This dependence can tentatively be explained as follows. The pump intensity is the highest in the central part of the pumped region, where it is kept approximately the same for all values of D . Let us assume that radiation propagates from each section of the outer boundary of the pumped region along the diameter, and most of the way gain saturation takes place. Saturation in the one-dimensional case was considered in [3], while, to our knowledge, the two-dimensional case has not yet been discussed in publications. All rays that cross the pumped area along the diameter are focused at its center. For this reason, the emission intensity is maximum in the central part of the pumped region. As D increases, the heating of carriers in the pumped region by emission, which slows their cooling [7], is enhanced. The effect of this slowdown on the recombination rate averaged over the saturated region is stronger than the effect of saturable amplification of the emission. This is evidenced by a decrease in I_{s-max} with an increase in D . However, the recombination rate in the central part will increase until $D < D_b$, because the increase in the area of the active region resulting from an increase in D leads to an additional contribution to the emission intensity at the focus. For $D < D_b$, this contribution prevails over emission attenuation caused by enhanced carrier heating, discussed above. The increase in the emission intensity, and, thus, in the recombination rate, in the central part of the pumped spot taking place in this way as D increases to D_b explains the decrease in n_{max} . For $D > D_b$, the decrease in the emission intensity due to carrier heating becomes dominant even in the central part of the pumped region. Therefore, the rate of stimulated recombination decreases and n_{max} increases accordingly with increasing D .

It was found that the width $\Delta\hbar\omega$ of the emission spectrum varies with D in the same way as $n_{max}(D)$ (Fig. 6), which demonstrates the relation between the width of the light amplification spectrum and the

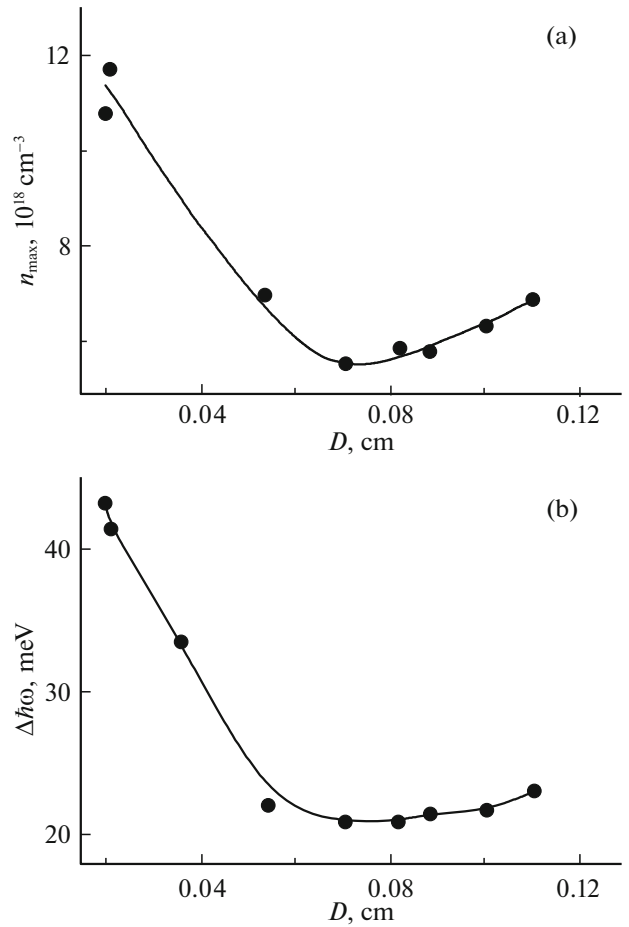


Fig. 6. Dependences of (a) the maximum carrier density n_{max} and (b) the width of the emission spectrum $\Delta\hbar\omega$ on the beam diameter D . Solid lines are drawn as guides to the eye.

maximum carrier density n_{max} . The much weaker increase in $\Delta\hbar\omega$ with D in the region of $D > D_b$ is apparently caused by the fact that the maximum carrier temperature T_{max} should also increase with n_{max} due to their mentioned interrelation.

Let us recall that the cooling of carriers means that they undergo intraband transitions (transport) to lower-lying energy levels, and the shorter the temperature relaxation time τ_T the more intense (rapid) the energy transport of carriers. This transport occurs both during the pulse that pumps the carriers and after the pulse while nonequilibrium carriers relax. When emission is so intense that it affects its own amplification (this is the so-called gain saturation stage), an increase in D at a constant pump energy density leads, as we can now suggest, to the following. At some value of D , the rates of the energy transport of carriers (averaged over the pumped region) to the extrema of the conduction and valence bands (from where they recombine) and the stimulated recombination of carriers attain their limiting values. Correspondingly,

emission amplification also attains its limiting level. This conclusion follows from the observed nonmonotonic behavior of the dependence $n_{\max}(D)$. According to the remaining experimental results of this study and those reported in [1], a further increase in D leads to a reduction in the energy-transport and stimulated recombination rates and a decrease in emission amplification. This gives evidence that there exists a self-maintaining balance between the rates of stimulated radiative recombination and energy transport of carriers. The latter process slows down due to the heating of carriers by emission, which increases the carrier cooling time τ_T . Balance is maintained automatically by emission, which regulates the depletion of the inverse population of the electron energy levels in the conduction band. This depletion was observed in [5].

4. CONCLUSIONS

Let us summarize. The maximum intensity of intrinsic stimulated picosecond emission from GaAs decreases as the pump-beam diameter D increases (while the pump energy density is fixed), contrary to what is expected according to the Bouguer law of linear optics. This dependence anticorrelates with the dependence of the characteristic relaxation time of emission on the diameter D . This time is proportional to the characteristic charge-carrier cooling time, which therefore, also anticorrelates with the maximum emission intensity. As D increases, the maximum carrier density n_{\max} (in the central part of the pumped region) and the width of the emission spectrum change with D in a similar nonmonotonic way, which is caused by the relation between the width of the light amplification spectrum and the maximum carrier density n_{\max} .

The observed phenomena occur under so-called gain saturation conditions, i.e., when the emitted radiation affects its own amplification. This is confirmed, for example, by depletion of the inverse population of electron energy levels in the conduction band as a result of the emission process, or, in other words, the formation of a dip in the region of the absorption spectrum corresponding to light amplification [5]. Depletion acts to maintain the balance between the rate of the stimulated radiative recombination of carriers and energy transport of carriers toward the extrema of the conduction and valence bands, from where they recombine. As D increases, the heating of carriers by emission is enhanced, which slows down their cooling and, accordingly, slows their energy transport. If the balance between recombination and carrier transport

is maintained, transport slowdown leads to a decrease in the emission intensity and to slowing down emission relaxation. Thus, we have shown the impact of the energy transport of carriers on the emission generation under the conditions of gain saturation. The transition from the unsaturated regime to gain saturation is manifested, in particular, in the nonmonotonic change of the carrier density n_{\max} with D .

It should be noted that we have revealed another implication of the energy transport of carriers important in the situation of intense picosecond emission, this time for stimulated recombination. Previously, we observed the slowdown of the healing of deviations from the Fermi distribution of charge carriers caused by this transport [9] and the formation of LO-phonon oscillations in the electron energy distribution caused by the energy transport of electrons assisted by the emission of LO phonons [5, 10].

FUNDING

This study was carried out in the framework of a state assignment.

CONFLICT OF INTEREST

The authors declare no conflict of interest.

REFERENCES

1. N. N. Ageeva, I. L. Bronevoi, D. N. Zabegaev, and A. N. Krivosov, *Semiconductors* **53**, 1431 (2019).
2. E. O. Goebel, O. Hildebrand, and K. Lohnert, *IEEE J. Quantum Electron.* **13**, 848 (1977).
3. L. W. Casperson, *J. Appl. Phys.* **48**, 256 (1977).
4. G. S. Landsberg, *Optics* (Nauka, Moscow, 1976) [in Russian].
5. N. N. Ageeva, I. L. Bronevoi, A. N. Krivosov, S. E. Kumekov, and S. V. Stegantsov, *Semiconductors* **36**, 136 (2002).
6. Yu. D. Kalafati and V. A. Kokin, *Sov. Phys. JETP* **72**, 1003 (1991).
7. S. E. Kumekov and V. I. Perel', *Sov. Phys. JETP* **67**, 193 (1988).
8. J. S. Blakemore, *J. Appl. Phys.* **53**, R123 (1982).
9. N. N. Ageeva, I. L. Bronevoi, D. N. Zabegaev, and A. N. Krivosov, *J. Commun. Technol. Electron.* **63**, 1235 (2018).
10. I. L. Bronevoi, A. N. Krivosov, and V. I. Perel', *Solid State Commun.* **94**, 805 (1995).

Translated by M. Skorikov